Phytochemistry 117 (2015) 363–372

Contents lists available at ScienceDirect

Phytochemistry

journal homepage: www.elsevier.com/locate/phytochem

Molecular and biochemical characterization of the UDP-glucose: Anthocyanin 5-*O*-glucosyltransferase from *Vitis amurensis*

Fei He [a,1], Wei-Kai Chen [a,1], Ke-Ji Yu [a], Xiang-Nan Ji [a], Chang-Qing Duan [a], Malcolm J. Reeves [a,b], Jun Wang [a,*]

[a] Center for Viticulture & Enology, College of Food Science and Nutritional Engineering, China Agricultural University, Beijing 100083, China
[b] Institute of Food, Nutrition and Human Health, Massey University, Palmerston North 4442, New Zealand

ARTICLE INFO

Article history:
Received 4 August 2014
Received in revised form 12 June 2015
Accepted 22 June 2015

Keywords:
Amur grape
Vitis amurensis
Vitaceae
Bis-glucosidic anthocyanin
UDP-glucose: anthocyanin 5-*O*-glucosyltransferase
Enzymology
Subcellular localization

ABSTRACT

Generally, red *Vitis vinifera* grapes only contain monoglucosidic anthocyanins, whereas most non-*vinifera* red grapes of the *Vitis* genus have both monoglucosidic and bis-glucosidic anthocyanins, the latter of which are believed to be more hydrophilic and more stable. Although previous studies have established the biosynthetic mechanism for formation of monoglucosidic anthocyanins, less attention has been paid to that of bis-glucosidic anthocyanins. In the present research, the full-length cDNA of UDP-glucose: anthocyanin 5-*O*-glucosyltransferase from *Vitis amurensis* Rupr. cv. 'Zuoshanyi' grape (Va5GT) was cloned. After acquisition and purification of recombinant Va5GT, its enzymatic parameters were systematically analyzed *in vitro*. Recombinant Va5GT used malvidin-3-*O*-glucoside as its optimum glycosidic acceptor when UDP-glucose was used as the glycosidic donor. Va5GT-GFP was found to be located in the cytoplasm by analyzing its subcellular localization with a laser-scanning confocal fluorescence microscope, and this result was coincident with its metabolic function of modifying anthocyanins in grape cells. Furthermore, the relationship between the transcriptional expression of *Va5GT* and the accumulation of anthocyanidin bis-glucosides during berry development suggested that Va5GT is a key enzyme in the biosynthesis of bis-glucosidic anthocyanins in *V. amurensis* grape berries.

1. Introduction

Accumulated widely in almost all plant organs, including roots, stems, leaves, flowers, berries and seeds, anthocyanins are a group of water-soluble flavonoid pigments synthesized from phenylalanine-derived plant secondary metabolites (Mazza, 1995; Winkel-Shirley, 2001). Normally, in pink, red, purple and black grapes, the accumulation of anthocyanins in berry skins determines the color of the grapes. The anthocyanin composition and content of red grapes are affected by various intrinsic factors, such as species and varieties, and many external factors, which results in noticeable differences between different grape varieties (Downey et al., 2006). Therefore, in the past several decades, much research has focused on anthocyanin biosynthesis in grapes.

The biosynthetic pathways to anthocyanins in various plants have been presented in detail in previous reports (Heller and Forkmann, 1993). Anthocyanins are first visible in grapes when the berries begin to expand at the start of veraison, and this occurs simultaneously with the rapid accumulation of sugar (Hrazdina et al., 1984). Anthocyanins are formed by a sequence of metabolic steps that can be divided into two different stages of reactions: production of anthocyanidin-3-*O*-glucosides (**2**, **4**, **6**, **8**, **10**, **12**) in Fig. 1, and further modifications of those glucosides (Martin et al., 1993). Generally, the glycosylation of an anthocyanidin or anthocyanin is catalyzed by uridine diphosphate glycosyltransferases (UGTs), which are characterized by a signature motif, the conserved plant secondary product glycosyltransferase box (PSPG) (Hughes and Hughes, 1994). This sugar conjugation modifies the anthocyanin, giving it increased water solubility and chemical stability, which could also facilitate the transfer of anthocyanins from their cytoplasmic production site into vacuoles, where anthocyanins finally accumulate (Nakatsuka et al., 2008). It is believed that anthocyanidins are first glycosylated at the 3-*O*-position by UDP-glucose: flavonoid 3-*O*-glucosyltransferase (3GT) to form their corresponding monoglucosidic anthocyanins. Then, the bis-glucosidic anthocyanins can be synthesized by the action of another member of the UGT family, UDP-glucose: anthocyanin 5-*O*-glucosyltransferase (5GT). To date, the genes encoding 3GTs

* Corresponding author at: Center for Viticulture & Enology, College of Food Science and Nutritional Engineering, China Agricultural University, No. 17 Tsinghua East Road, Beijing 100083, China.
E-mail address: jun_wang@cau.edu.cn (J. Wang).
[1] These authors contributed equally to this work.

http://dx.doi.org/10.1016/j.phytochem.2015.06.023
0031-9422/

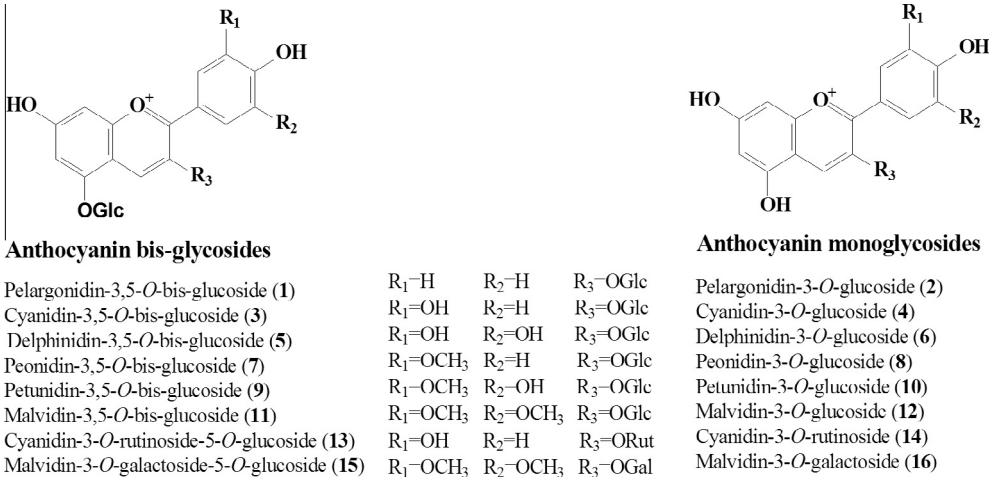

Fig. 1. Chemical structure of anthocyanidin monoglycosides (**2**, **4**, **6**, **8**, **10**, **12**, **14**, **16**) and their corresponding bis-glycosides (**1**, **3**, **5**, **7**, **9**, **11**, **13**, **15**). Glc, Rut and Gal are abbreviations for glucoside, rutinoside and galactoside, respectively.

have been isolated and well characterized in several different grape species and varieties (Ford et al., 1998; Hall et al., 2012; Offen et al., 2006; Sparvoli et al., 1994). However, only a few studies have reported the isolation of *5GT* genes or their enzymes from a limited number of grape germplasms (Jánváry et al., 2009; Neumann et al., 2006). Jánváry et al. (2009) cloned two *5GT* alleles (functional *Cha5GT* and nonfunctional *Dia5GT*) from the heterozygous hybrid cultivar 'Regent', which is a cross of *V. vinifera* cv. 'Diana' and the interspecific hybrid cv. 'Chambourcin'. A functional analysis of Cha5GT and Dia5GT established that two mutations in the *5GT* gene disrupt its enzymatic activity. Because of the absence of active 5GT in *V. vinifera* red grapes, they only accumulate anthocyanidin monoglucosides (**2**, **4**, **6**, **8**, **10**, **12**), but not their corresponding bis-glucosides (**1**, **3**, **5**, **7**, **9**, **11**), which are widely found in the mature red grapes of almost all non-*vinifera* species (Mazzuca et al., 2005).

In recent years, *V. amurensis* grapes have been the focus of several studies, particularly with regards to their ability to produce resveratrol and their cold hardiness and fungal disease resistance (Kiselev et al., 2007; Kovács et al., 2003; Wan et al., 2007). Unlike *V. vinifera* grapes, the berry skins of *V. amurensis* species usually accumulate abundant anthocyanidin-3,5-*O*-bis-glycosides (**1**, **3**, **5**, **7**, **9**, **11**), due to their highly active 5GT (He et al., 2010a). However, little has been reported on the gene sequences and biochemical functions of 5GT from *V. amurensis* grapes, and no thorough enzymatic characterization of a grape 5GT has been reported previously.

In this study, the full-length cDNA sequence of *Va5GT* from *V. amurensis* Rupr. cv. 'Zuoshanyi' was cloned and used for heterologous expression of the Va5GT protein for its biochemical characterization. A green fluorescent protein (GFP)-tagged Va5GT protein was also localized in *Arabidopsis* leaf cell protoplasts, as determined by laser scanning confocal microscopy. Furthermore, the comparison of *Va5GT* transcriptional expression and the resulting accumulation of bis-glucosidic anthocyanins (**3**, **5**, **7**, **9**, **11**) in grape skins during berry development showed that Va5GT is the crucial structural enzyme in the biosynthesis of bis-glucosidic anthocyanins in these grapes.

2. Results and discussion

2.1. Molecular cloning and bioinformatics analysis of Va5GT

The oligonucleotide primers used in the previous study of *Cha5GT* were selected to amplify *Va5GT* (Jánváry et al., 2009). A nucleotide sequence analysis demonstrated that the full-length *Va5GT* (Genbank accession KF996717) contained an open reading frame of 1395 bp, which was in 99.6% agreement with the previously characterized gene *Cha5GT* (the nucleotide sequence of *Cha5GT* were offered by Prof. Schwab). Thus, *Cha5GT* and *Va5GT* could be considered homologous genes from different grape species. The ExPASy website (http://web.expasy.org/compute_pi/) was used to analyze the encoded amino acid sequence of *Va5GT*, and the Va5GT protein had an estimated isoelectric point of 5.12 and a predicted molecular weight of 51.5 kDa.

An analysis of the Va5GT amino acid sequence using the Pfam 24.0 website (http://pfam.sanger.ac.uk/search/sequence) showed that Va5GT belongs to the GT-B clan of the UGTs family, which contains a diversity of glycosyltransferases (Coutinho et al., 2003). Based on the amino acid sequences of various functionally characterized plant glucosyltransferases that are related to anthocyanin biosynthesis and of the obtained Va5GT, a neighbor-joining phylogenetic tree was constructed. As shown in Fig. 2, three clusters were generally grouped based on *in vitro* regio-selectivity rather than substrate specificity, and Va5GT was placed in cluster II (Vogt and Jones, 2000). In this phylogenetic tree, cluster I exclusively contained flavonoid 3-*O*-glycosyltransferases. Cluster II mainly included anthocyanin 5-*O*-glycosyltransferases and some flavonol 7-*O*-glucosyltransferases. Among them, Va5GT exhibited 40.9–55.5% identities with 5GTs with similar biochemical functions in other plants. The enzymes in cluster III could potentially catalyze the second glycosylation of other anthocyanins or flavonoid glycosides, and usually used a glycosidic donor other than UDP-glucose. For example, the recombinant UDP-xylose: anthocyanidin-3-*O*-galactoside 2″-*O*-xylosyltransferase (AcA3Ga2″XT) from *Actinidia chinensis* catalyzed the production of cyanidin-3-*O*-xylo-galactoside using cyanindin-3-*O*-galactoside and UDP-xylose as substrates (Montefiori et al., 2011).

The alignment of the protein sequences of Va5GT and other glucosyltransferases in grapes showed that Va5GT contained a common C-terminal domain of the UGT superfamily (Fig. S1). Glutamine and histidine residues were highly conserved as the last amino acid residues of the PSPG boxes in glucosyltransferases and galactosyltransferases, respectively. The glutamine residue at the end of the PSPG box in Va5GT suggested that Va5GT might use UDP-glucose as its sugar donor rather than UDP-galactose (Kubo et al., 2004). A previous study confirmed that a truncation at the C-terminus and a V110L transition in Vv5GT disrupted its enzymatic activity in the production of anthocyanin-3,5-*O*-bis-glucosides (Jánváry et al., 2009). Fortunately, the protein sequence

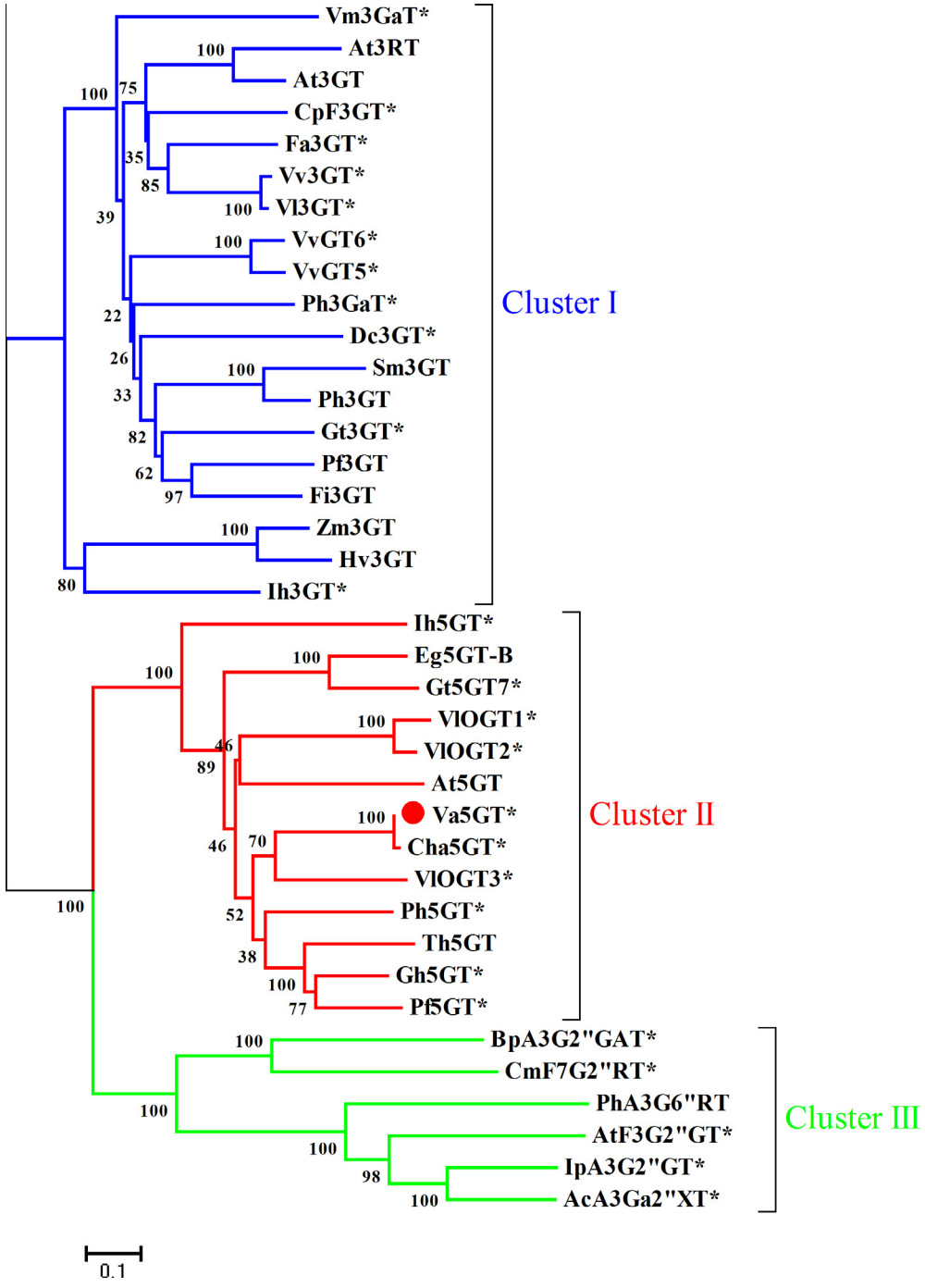

Fig. 2. Neighbor joining phylogenetic tree analysis of various plant glycosyltransferases including Va5GT. Asterisks indicate glycosyltransferases that have been biochemically characterized. Numbers next to branches indicate bootstrap percentages out of 1000 replicates. Scale bars indicate an evolutionary distance of 0.1 amino acid substitutions per position in the sequence. Abbreviations: At3RT, *Arabidopsis thaliana* flavonol 3-*O*-rhamnosyltransferase (NP_564357); Ph3GaT, *Petunia hybrida* flavonoid 3-*O*-galactosyltransferase (AAD55985); Vm3GaT, *Vigna mungo* flavonoid 3-*O*-galactosyltransferase (BAA36972); At3GT, *A. thaliana* UDP-glucose: flavonoid 3-*O*-glucosyltransferase (CAC01718); CpF3GT, *Citrus* × *paradisi* flavonol 3-*O*-glucosyltransferase (ACS15351); Dc3GT, *D. caryophyllus* flavonoid 3-*O*-glucosyltransferase (BAD52005); Fa3GT, *Fragaria* × *ananassa* UDP-glucose glucosyltransferase (AAU09442); Fi3GT, *Forsythia intermedia* flavonoid 3-*O*-glucosyltransferase (AAD21086); Gt3GT, *Gentiana triflora* flavonoid 3-*O*-glucosyltransferase (BAA12737); Hv3GT, *Hordeum vulgare* flavonoid 3-*O*-glucosyltransferase (CAA33729); Ih3GT, *Iris hollandica* anthocyanidin 3-*O*-glucosyltransferase (BAD83701); Ph3GT, *P. hybrida* flavonoid 3-*O*-glucosyltransferase (BAA89008); Pf3GT, *Perilla frutescens* flavonoid 3-*O*-glucosyltransferase (BAA19659); Sm3GT, *Solanum melongena* flavonoid 3-*O*-glucosyltransferase (CAA54558); Vv3GT, *V. vinifera* flavonoid 3-*O*-glucosyltransferase (AAB81683); Vl3GT, *V. labrusca* flavonoid 3-*O*-glucosyltransferase (ABR24135); VvGT5, *V. vinifera* UDP-glucuronic acid: flavonol-3-*O*-glucuronosyltransferase (BAI22846); VvGT6, *V. vinifera* flavonol bifunctional glucosyl/galactosyl-transferase (BAI22847); At5GT, *A. thaliana* anthocyanin 5-*O*-glucosyltransferase (NP_193146); Cha5GT, *Vitis* cv. 'Regent' anthocyanin 5-*O*-glucosyltransferase; Eg5GT-B, *Eustoma grandiflorum* anthocyanin 5-*O*-glucosyltransferase (BAF49286); Gh5GT, *Glandularia* × *hybrida* UDP-glucose: anthocyanin 5-*O*-glucosyltransferase (BAA36423); Gt5GT7, *G. triflora* anthocyanin 5-*O*-glucosyltransferase (BAG32255); Ih5GT, *I. hollandica* anthocyanin 5-*O*-glucosyltransferase (BAD06874); Ph5GT, *P. hybrida* anthocyanin 5-*O*-glucosyltransferase (BAA89009); Pf5GT, *P. frutescens* anthocyanin 5-*O*-glucosyltransferase (BAA36421); Th5GT, *Torrenia hybrida* anthocyanin 5-*O*-glucosyltransferase (BAC54093); Va5GT, *V. amurensis* anthocyanin 5-*O*-glucosyltransferase (AHL68667); VlOGT1, *V. labrusca O*-glucosyltransferase 1 (ABQ02256); VlOGT2, *V. labrusca O*-glucosyltransferase 2 (ABQ02257); VlOGT3, *V. labrusca O*-glucosyltransferase 3 (ABQ02258); AcA3Ga2″XT, *Actinidia chinensis* UDP-xylose: anthocyanidin-3-*O*-galactoside 2″-*O*-xylosyltransferase (FG404013); AtF3G2″, *A. thaliana* flavonol 3-*O*-glucoside 2″-*O*-glucosyltransferase (NP_200212); BpA3G2″GAT, *Bellis perennis* UDP-glucuronic acid: anthocyanidin-3-*O*-glycoside 2″-*O*-glucuronosyltransferase (BAD77944); CmF7G2″RT, *Citrus maxima* UDP-rhamnose:flavonoid-7-*O*-glycoside 1,2-*O*-rhamnosyltransferase (AAL06646); IpA3G2″GT, *Ipomoea purpurea* UDP-glucose: anthocyanidin-3-*O*-glucoside 2″-*O*-glucosyltransferase (BAD95882); PhA3G6″RT, *P. hybrida* UDP-rhamnose:anthocyanidin-3-*O*-glycoside 1,6-*O*-rhamnosyltransferase (CAA50376).

alignment showed that Va5GT shared the same sequences with those of the functional Cha5GT protein at these two mutation sites, which suggested that the recombinant Va5GT expressed in our experiments would actively function in the glycosylation of anthocyanins at the 5-*O*-position.

2.2. Expression in vitro and enzyme activity of recombinant Va5GT

The recombinant vector pET32a-*Va5GT* was introduced into *Escherichia coli* Rosetta (DE3) cells and expressed under isopropyl-β-*D*-thiogalactoside (IPTG) induction. SDS–PAGE analysis showed a 70 kDa band, which was precisely equal to the expected molecular mass of the Va5GT protein (54 kDa) fused to the pET32a Tag protein (16 kDa), which included thioredoxin, His-tag, S-tag and enterokinase moieties (Fig. 3). Expression of the recombinant protein yielded approximately 0.66 mg of Va5GT fusion protein per liter of culture.

Substrate specificity studies for the recombinant Va5GT protein were performed by testing UDP-glucose and UDP-galactose as donors with different monoglycosidic anthocyanins as acceptors. When UDP-glucose was used as the sugar donor, recombinant Va5GT could further catalyze 5-*O*-glucosylation of almost all of the tested anthocyanidin-3-*O*-glucosides, including pelargonidin-3-*O*-glucoside (**2**), cyanidin-3-*O*-glucoside (**4**), delphinidin-3-*O*-glucoside (**6**), peonidin-3-*O*-glucoside (**8**), petunidin-3-*O*-glucoside (**10**) and malvidin-3-*O*-glucoside (**12**) (Fig. 4). Recombinant Va5GT could also catalyze the glycosylation of some anthocyanins that are not normally found in grapes, including malvidin-3-*O*-galactoside (**16**) and cyanidin-3-*O*-rutinoside (**14**), as shown in Fig. 4. Furthermore, recombinant Va5GT could not use UDP-galactose as a sugar donor substrate, which was consistent with our prediction and was similar to the property of anthocyanin 5-*O*-glucosyltransferase extracted from flowers of *Dahlia variabilis* (Ogata et al., 2001).

The results of the substrate selectivity analysis of recombinant Va5GT for various anthocyanidin-3-*O*-monoglycosides showed that it preferentially glucosylated malvidin-3-*O*-glucoside (**12**), petunidin-3-*O*-glucoside (**10**) and peonidin-3-*O*-glucoside (**8**) rather than cyanidin-3-*O*-glucoside (**4**) or delphinidin-3-*O*-glucoside (**6**) (Table 1). The relative activity of recombinant Va5GT with *O*-methoxylated anthocyanins was apparently higher than with their hydroxylated counterparts, which was in agreement with results reported for 3GT from *V. labrusca* cv. 'Concord' (Vl3GT) but not for results reported for 3GT from *V. vinifera* L. cv. 'Shiraz' (Vv3GT) (Ford et al., 1998; Hall et al., 2012). This substrate specificity of recombinant Va5GT is in accordance with the anthocyanin composition of *V. amurensis* Rupr. cv. 'Zuoshanyi', which is dominated by methylated bis-glucosidic anthocyanins, especially malvidin-3,5-*O*-bis-glucoside (**11**). The relative activity of Va5GT with cyanidin-3-*O*-rutinoside (**14**) was quite similar to that with cyanidin 3-*O*-glucoside (**4**) (only 3% lower), but the relative activity of Va5GT with malvidin-3-*O*-galactoside (**16**) was much higher (approximately 28% higher) than that with malvidin-3-*O*-glucoside (**12**) (Table 1). These results are of interest because these two non-glucosidic anthocyanins are not detected in grapes, and Va5GT was able to tolerate the galactose and rutinose groups in the 3-*O*-position of those anthocyanins. This suggests that the relative activities of recombinant Va5GT with sugar acceptors was largely dependent on the structure of the aglycones, especially the flavonoid B ring methylation configuration, rather than on glycoside type.

The optimum reaction conditions for recombinant Va5GT with malvidin-3-*O*-glucoside (**12**) and UDP-glucose were determined. The optimum reaction temperature was 25 °C, and the optimum pH value was 7.0 (Fig. S2), which is equal to the pH in the cytoplasm of grape cells (Felle, 2005; Hall and De Luca, 2007). Furthermore, the addition of 10 mM Fe^{2+}, Mg^{2+} or Ca^{2+} had only a slight effect on the reaction, whereas the addition of 10 mM Cu^{2+} completely inhibited the activity of recombinant Va5GT. In contrast, Na^{+} at the same concentration was shown to slightly increase the activity of recombinant Va5GT. The addition of benzoic acid at 10 mM reduced the activity of recombinant Va5GT, but imidazole at the same concentration had almost no effect (Table S1). These observations were quite similar to those reported earlier for enzymes of the UGT family (Ford et al., 1998; Owens and McIntosh, 2009). The results also indicated that diethylpyrocarbonate (DEPC) could disrupt glucosyltransferase activity, possibly through the covalent modification of histidine residues (Owens and McIntosh, 2009).

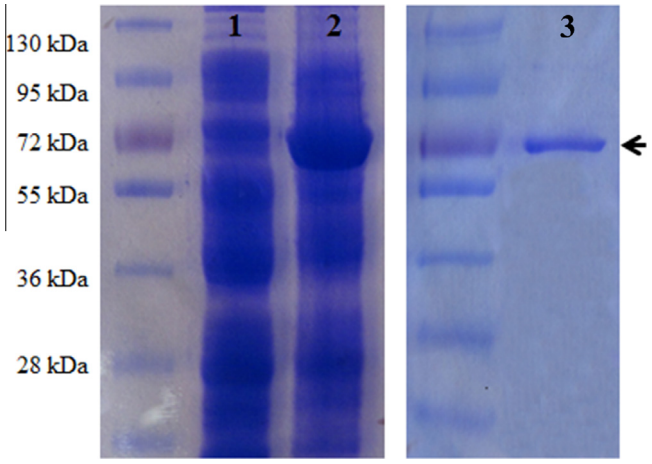

Fig. 3. SDS–PAGE analysis of the expressed products of pET32a-*Va5GT* by Coomassie Brilliant Blue R250 staining. Lane 1, uninduced cells; Lane 2, induced cells; Lane 3, purified recombinant Va5GT after Ni–NTA affinity chromatography.

Under kinetic analysis conditions, recombinant Va5GT catalyzed conversion of malvidin-3-*O*-glucoside (**12**) to its 5-*O*-glucoside (**11**) at a linear rate for 10 min (Fig. S3). The saturation kinetics analysis of recombinant Va5GT gave an apparent Michaelis–Menten constant (K_m) for malvidin-3-*O*-glucoside (**12**) of 80.9 μM, a maximal velocity (V_{max}) value for malvidin-3,5-*O*-bis-glucoside (**11**) formation of 3.98 nKatals mg^{-1}, an apparent k_{cat} value of 0.279 s^{-1}, and a calculated catalytic efficiency of 3.45×10^3 M^{-1} s^{-1} (Fig. S4A). For the donor substrates, an apparent K_m value for UDP-glucose of 0.213 mM and a V_{max} value of 4.62 nKatals mg^{-1} were obtained (Fig. S4B). These results were similar to the biochemical properties (K_m values of 29.5 μM for delphinidin-3-*O*-glucoside (**6**) and 3.4 μM for malvidin-3-*O*-glucoside (**12**)) of a recombinant Gt5GT7 protein obtained from *G. triflora*, which was heterologously expressed in bacteria cells (Nakatsuka et al., 2008). In a previous report, the corresponding K_m values of a recombinant Pf5GT from *Perilla frutescens* were 31.4 μM and 0.94 mM for cyanidin-3-*O*-glucoside (**4**) and UDP-glucose, respectively (Yamazaki, 1999). Additionally, an apparent k_{cat} value of 0.323 s^{-1} and a k_{cat}/K_m value of 1.52×10^3 M^{-1} s^{-1} were also found for the recombinant Pf5GT, and these are rational values and are similar to values reported previously by the Bowles group for Arabidopsis glycosyltransferases (Cartwright et al., 2008). However, no reports of kinetic parameters for 5GTs from grapes were found.

Moreover, the corresponding kinetic parameters of a recombinant Vv3GT (K_m values of 30 μM for cyanidin and 1.88 mM for UDP-glucose, k_{cat}/K_m value of 1.59×10^6 M^{-1} s^{-1} for cyanidin) and a recombinant Vl3GT (K_m values of 4.8 μM for cyanidin and 0.91 mM for UDP-glucose, k_{cat}/K_m values of 146 M^{-1} s^{-1} for cyanidin and 0.27 M^{-1} s^{-1} for UDP-glucose) were previously reported (Ford et al., 1998; Hall et al., 2012). The results here for the kinetic

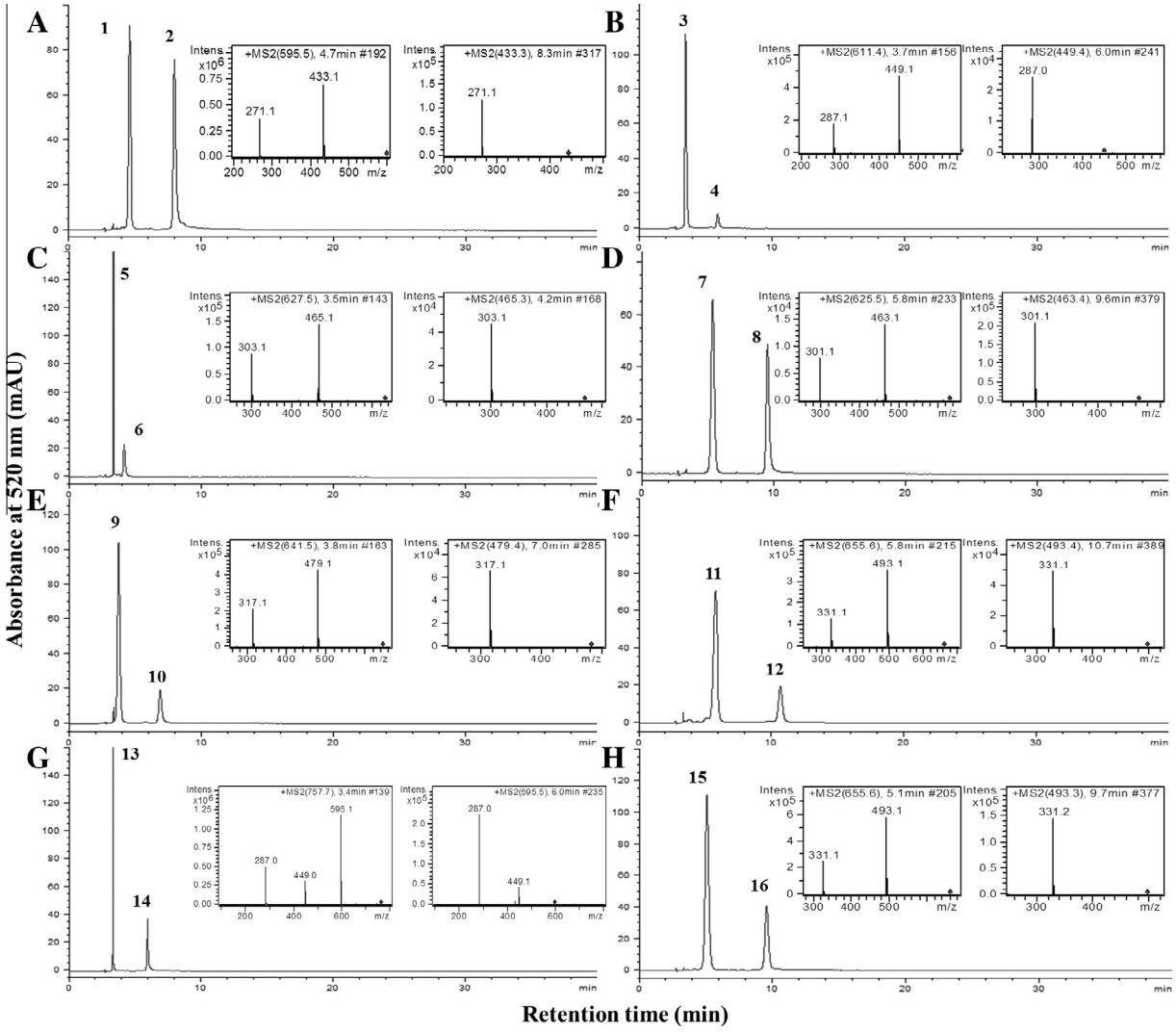

Fig. 4. HPLC–ESI–MS/MS analysis of products from the reactions *in vitro*. The substrates were as follows: (A), pelargonidin-3-*O*-glucoside (**2**); (B), cyanidin-3-*O*-glucoside (**4**); (C), delphinidin-3-*O*-glucoside (**6**); (D), peonidin-3-*O*-glucoside (**8**); (E), petunidin-3-*O*-glucoside (**10**); (F), malvidin-3-*O*-glucoside (**12**); (G), cyanidin-3-*O*-rutinoside (**14**) and (H), malvidin-3-*O*-galactoside (**16**). The chromatogram of the reaction of recombinant Va5GT enzyme (2.5 μg) with 1 mM UDP-glucose and 0.5 mM acceptor substrate for 20 min is shown with detection by absorbance at 525 nm. The insets show the mass spectra of the product and the substrate, respectively.

Table 1
Substrate selectivity of recombinant Va5GT for sugar acceptors.

Substrate	Authentic standard product	Relative activity[a] (%)
Malvidin-3-*O*-glucoside (**12**)	Malvidin-3,5-*O*-bis-glucoside (**11**)	100
Cyanidin-3-*O*-glucoside (**4**)	Cyanidin-3,5-*O*-bis-glucoside (**3**)	67
Delphinidin-3-*O*-glucoside (**6**)	Not used	62
Peonidin-3-*O*-glucoside (**8**)	Peonidin-3,5-*O*-bis-glucoside (**7**)	77
Petunidin-3-*O*-glucoside (**10**)	Not used	87
Pelargonidin -3-*O*-glucoside (**2**)	Not used	83
Cyanidin-3-*O*-rutinoside (**14**)	Not used	64
Malvidin-3-*O*-galactoside (**16**)	Not used	128

[a] All reported values are relative to that of malvidin-3-*O*-glucoside (**12**).

parameters of the recombinant Va5GT generated here were just within the reasonable range based on previously reported results. The synchronous catalysis efficiency of these enzymes involved in the anthocyanin biosynthetic pathway might be important for the accumulation of anthocyanins in grape berries because previous studies have suggested that the key structural enzymes of this metabolism might form a multi-enzyme complex and execute their functions together (Hrazdina and Wagner, 1985; Winkel-Shirley, 1999, 2004).

2.3. Subcellular localization of Va5GT in vivo

The analysis of the amino acid sequence of Va5GT using TargetP 1.1 (http://www.cbs.dtu.dk/services/TargetP/) assigned a predicted localization of "other" instead of "chloroplast", "mitochondrial" and "signal peptide". The prediction of the structure of Va5GT by TMHMM v 2.0 (http://www.cbs.dtu.dk/services/TMHMM/) and SignalP 4.1 (http://www.cbs.dtu.dk/services/SignalP/) showed no transmembrane helix and no signal peptide for transfer to the

secretory pathway (Emanuelsson et al., 2007). These predictions supported the results of our subsequent research, as Va5GT was found localized in the cytoplasm.

To experimentally investigate the subcellular localization of Va5GT, the pEZS-NL-*Va5GT* recombinant vector was constructed and introduced into *A. thaliana* protoplasts by polyethylene glycol (PEG)-Ca^{2+} mediated transient transformation. The recombinant Va5GT protein was GFP-tagged downstream and was found to be distributed evenly in the cytosolic space; no green fluorescence was observed in chloroplasts and other cellular organelles, as shown in Fig. 5A–C.

To further verify the subcellular localization of Va5GT, PYRABACTIN RESISTANCE 1 (PYR1) tagged with mCherry (a red fluorescent protein, RFP) was used as a positive marker. PYR1 is a member of the START family of proteins (called PYR/PYL/RCAR) and is an ABA receptor that can localize in the cytoplasm (Park et al., 2009; Zhao et al., 2011). Co-transformation of *A. thaliana* protoplasts with the pMD19-T-*PYR1* and pEZS-NL-*Va5GT* vectors resulted in nearly complete co-localization of PYR1 and Va5GT recombinant proteins in the cytosol, as shown in Fig. 5D–F.

In previous research, flavanone synthase, chalcone isomerase and 3GT were investigated in intact protoplasts and in cytoplasmic and vacuolar fractions. The cytoplasmic fraction showed the highest enzymatic activity, and the authors concluded that the cytosol was involved in anthocyanin biosynthesis (Hrazdina et al., 1978). It had been proposed that phenylpropanoid and flavonoid biosynthesis take place on enzyme complexes that are membrane-associated via protein–protein interactions (Hrazdina and Wagner, 1985; Winkel-Shirley, 1999, 2004). As anthocyanin 5-aromatic acyltransferase from *Gentiana triflora* and anthocyanin *O*-methyltransferase from *V. vinifera* have both been shown to localize in the cytoplasm, it seems reasonable that Va5GT would also localize in the cytosol (Fujiwara et al., 1998; Hugueney et al., 2009). Interestingly, Matsuba et al. (2010) suggested that the vacuole was a strong candidate location for DcAA5GT, which was different with the results here. This might be because Matsuba et al. studied carnation rather than grapevine, and these two plants may have different anthocyanin accumulation and translation models. DcAA5GT contains a putative transit peptide sequences that is necessary for localization in vacuoles, the optimum pH range for its enzymatic activity was 4.5–5.0, which is equal to the pH range inside vacuoles (Matsuba et al., 2010; Tanaka et al., 1998). In contrast, our recombinant Va5GT did not contain any signal peptide and had high activity from pH 7.0–8.0, which was corresponds with the pH values of the cytoplasm. Recombinant Va5GT was shown to localize in the cytosol, as is the case for most UGTs involved in anthocyanin biosynthesis (Yonekura-Sakakibara et al., 2009).

2.4. Identification and quantification of anthocyanins in berry skins of two V. amurensis cultivars

Using high performance liquid chromatography–electrospray ionization–tandem mass spectrometry (HPLC–ESI–MS/MS), anthocyanin components extracted from grape skins of 'Zuoshanyi' and 'Zuohongyi' were analyzed. In total, only 13 types of anthocyanins were identified from the berry skins of these two *V. amurensis* cultivars based on their retention time and MS/MS information. 5 non-acylated monoglucosidic anthocyanins and 5 non-acylated bis-glucosidic anthocyanins which are all known *Vitis* metabolites were detected (Zhao et al., 2010; Zhu et al., 2012). Furthermore, 3 unknown monoglucosidic anthocyanin derivatives were present in trace amounts (Table 2). No acylated monoglucosidic or bis-glucosidic anthocyanins were characterized, which might be due to the characteristics of the grape berries of the *V. amurensis* species (Zhao et al., 2010; Zhu et al., 2012). In 'Zuoshanyi', the total anthocyanin contents at 8, 10, and 12 weeks after flowering were 1.14, 3.27 and 5.62 mg/g in dry skin material, respectively. Meanwhile in 'Zuohongyi', the interspecific hybrid of *V. vinifera* and *V. amurensis*, the total anthocyanin contents at 8, 10, and 12 weeks after flowering were 1.99, 2.98 and 5.14 mg/g in dry skin material,

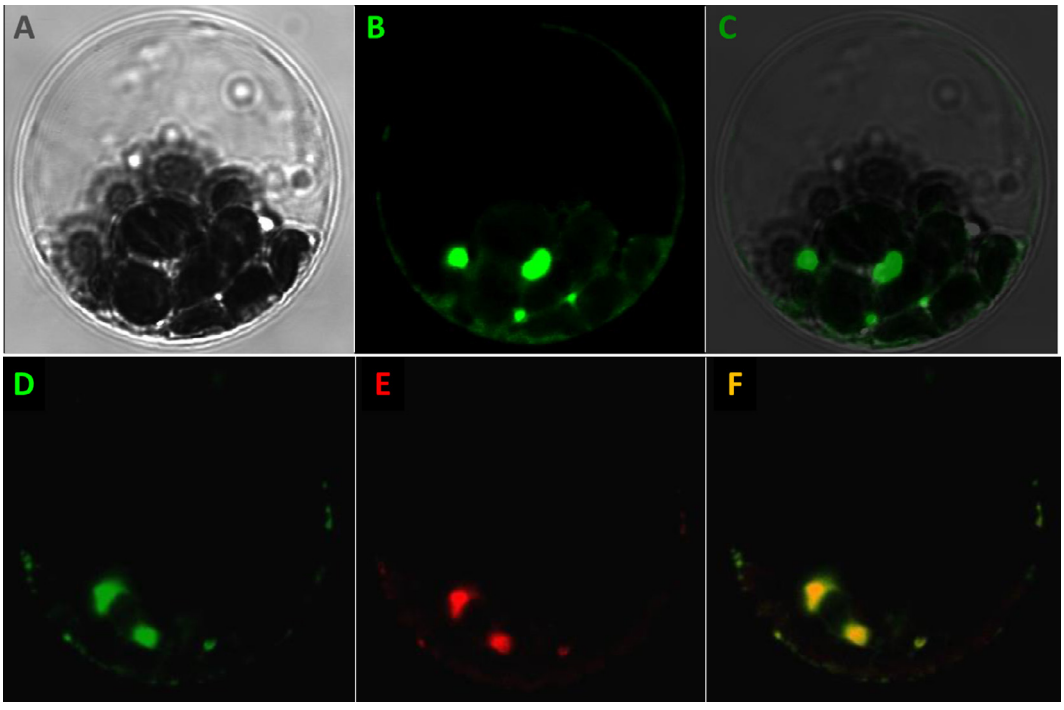

Fig. 5. Confocal laser scanning microscopy of transiently expressed Va5GT-GFP and PYR1-RFP fusion proteins in *A. thaliana* protoplasts. (A), light-microscopy image of intact protoplast; (B), fluorescence of Va5GT-GFP fusion protein; (C), merged images of A and B; (D), fluorescence of Va5GT-GFP fusion protein; (E), fluorescence of PYR1-RFP fusion protein; (F), merged images of D and E.

Table 2
Qualitative and quantitative analysis of anthocyanins in grape skins (mg/g dry skin material) of *V. amurensis* 'Zuoshanyi' (ZSY) and 'Zuohongyi' (ZHY) at harvest by HPLC–ESI–MS/MS.

No.	Anthocyanin	*Vitis* metabolites[a]	Authentic standard[b]	Retention time (min)	$[M]^+$ (*m/z*)	Fragment ion M^+ (*m/z*)	ZSY (mg/g)	ZHY (mg/g)
1	Delphinidin-3,5-*O*-bis-glucoside (**5**)	Y	–	2.81	627	465, 303	0.704 ± 0.094	0.171 ± 0.013
2	Cyanidin-3,5-*O*-bis-glucoside (**3**)	Y	+	3.49	611	449, 287	0.203 ± 0.043	0.096 ± 0.001
3	Petuinidin-3,5-*O*-bis-glucoside (**9**)	Y	–	3.71	641	479, 317	0.834 ± 0.154	0.344 ± 0.005
4	Dephinidin-3-*O*-glucoside (**6**)	Y	+	4.09	465	303	0.271 ± 0.068	1.944 ± 0.056
5	Peonidin-3,5-*O*-bis-glucoside (**7**)	Y	+	5.50	625	463, 301	0.801 ± 0.050	0.167 ± 0.004
6	Malvidin-3,5-*O*-bis-glucoside (**11**)	Y	+	5.71	655	493, 331	2.510 ± 0.088	0.707 ± 0.032
7	Cyanidin-3-*O*-glucoside (**4**)	Y	+	5.80	449	287	Trace	Trace
8	Petunidin-3-*O*-glucoside (**10**)	Y	+	6.83	479	317	0.066 ± 0.008	0.866 ± 0.003
9	Peonidin-3-*O*-glucoside (**8**)	Y	+	9.50	463	301	0.111 ± 0.023	0.158 ± 0.013
10	Malvidin-3-*O*-glucoside (**12**)	Y	+	10.60	493	331	0.118 ± 0.017	0.691 ± 0.001
11	Cyanidin derivative	N	–	12.70	477	287	Not detected	Trace
12	Petunidin derivative	N	–	13.10	507	317	Not detected	Trace
13	Malvidin derivative	N	–	19.10	521	331	Trace	Trace

[a] 'Y' indicates that the compound was known *Vitis* metabolites; 'N' indicates that the compound was not known *Vitis* metabolites.
[b] '+' indicates that the compound was identified using authentic standard; '–' indicates that the compound was not identified using authentic standard.

respectively. However, in these two cultivars, the total bis-glucosidic anthocyanin contents in dry skin material at the three different developmental stages were 0.99, 2.96 and 5.05 mg/g in 'Zuoshanyi' and 0.29, 0.54, 1.48 mg/g in 'Zuohongyi'. Among the identified anthocyanins, the most abundant at harvest were malvidin-3,5-*O*-bis-glucoside (**11**) for 'Zuoshanyi' and delphinidin-3-*O*-monoglucoside (**6**) for 'Zuohongyi'. The differences in anthocyanin composition and content in 'Zuoshanyi' and 'Zuohongyi' might be caused by the genetic differences of these two grape cultivars. Thus, it could be concluded that in the late developmental stages of grape berries, more bis-glucosidic anthocyanins (**3**, **5**, **7**, **9**, **11**) are biosynthesized and accumulated in these two cultivars and that the pure *V. amurensis* cultivar 'Zuoshanyi' can accumulate more bis-glucosidic anthocyanins than the related hybrid 'Zuohongyi'.

2.5. Expression of Va5GT and anthocyanin accumulation during grape berry development

In both cultivars, almost no expression of the *Va5GT* gene was detected in berry skins prior to veraison. After the beginning of veraison, the relative expression of the *Va5GT* gene in berry skins gradually increased and reached its highest level at the mature berry stage. At every developmental stage, the relative expression of *Va5GT* in 'Zuoshanyi' berry skins was higher than that in 'Zuohongyi', which is in agreement with the observed accumulation levels of bis-glucosidic anthocyanins in samples from these species, as shown in Fig. 6. Bis-glucosidic anthocyanins accounted for more than 86.8% (with a maximum of 90.5% at 10 weeks after flowering) of the total anthocyanins in all developmental stages of 'Zuoshanyi', whereas in 'Zuohongyi', bis-glucosidic anthocyanins never accounted for more than 28.8% (with a minimum of 14.6% at 8 weeks after flowering) of the total anthocyanins. This might be due to the genetic differences between these two grape cultivars; 'Zuoshanyi' is a homologous *V. amurensis* cultivar with high anthocyanin, especially bis-glucosidic anthocyanin biosynthesis, and in contrast, 'Zuohongyi' is a complex interspecific cross product of pure *V. amurensis* grapes and *V. vinifera* L. cv. 'Muscat Rouge de Frontignan' and exhibits poor anthocyanin accumulation. Thus, the lower relative expression of *Va5GT* and the lower bis-glucosidic anthocyanin accumulation in the 'Zuohongyi' cultivar was understandable.

Previously, Hall et al. (2012) detected the relative gene expression of *Vl3GT* in 'Concord' (*V. labrusca* L. cv.) grapes throughout grape berry development. They found little expression of *Vl3GT* in berry skins before veraison, but these transcripts began to accumulate at the beginning of veraison (8 weeks after flowering). The transcript level of *Vl3GT* continued to increase and reached its maximum value at 12 weeks after flowering, after which it decreased until harvest. This was similar to the results here, which further support the hypothesis that glycosyltransferases related to anthocyanin biosynthesis are only expressed after veraison and that their expression intensity increases during berry maturation.

Normally, *V. amurensis, V. labrusca* and other non-*vinifera* grapes consist not only of anthocyanidin monoglucosides but also of a great amount of bis-glucosides (Shewfelt and Ahmed, 1966). The amount of anthocyanidin bis-glucosides increased throughout grape berry development in 'Zuoshanyi' and 'Zuohongyi', and this result was in line with our expectation that Va5GT plays an important role in anthocyanin biosynthesis after veraison. The accumulation patterns for anthocyanidin bis-glucosides in the two grape cultivars were nearly identical. With berry maturation, the color of the grape skins deepened, and the level of anthocyanidin bis-glucosides reached its maximum by the time of berry maturity.

3. Conclusions

The molecular cloning, recombinant expression and *in vitro* biochemical characterization of Va5GT from 'Zuoshanyi' grape berries showed its ability to transfer sugar moieties from UDP-glucose to anthocyanidin-3-*O*-monoglycosides to synthesize bis-glucosidic anthocyanins. Substrate specificity studies indicate that Va5GT can use UDP-glucose as its exclusive glycosidic donor and a variety of anthocyanidin-3-*O*-monoglycosides, with a strong preference for malvidin-3-*O*-glucoside (**12**), as its glycosidic acceptors. Furthermore, the results of the subcellular localization study and real-time PCR analysis indicate that the expression of *Va5GT* coincided well with the accumulation of anthocyanidin-3,5-*O*-bis-glucosides (**3**, **5**, **7**, **9**, **11**) after veraison, suggesting that Va5GT plays an important role in the biosynthesis and accumulation of bis-glucosidic anthocyanins in *V. amurensis* grapes.

4. Experimental

4.1. Plant materials and chemicals

Five-year-old grapevines of 'Zuoshanyi' (*V. amurensis* Rupr., selected from wild resources, female) and 'Zuohongyi' [interspecific hybrid, female parent '79–26-58': 'Zuoshaner' (*V. amurensis* Rupr., selected from wild resources, female) × 'Muscat Rouge de Frontignan' (*V. vinifera* L., mutation of Muscat Blanc a Petits Grains), male parent: '74–6-83': '73121' (*V. amurensis* Rupr.,

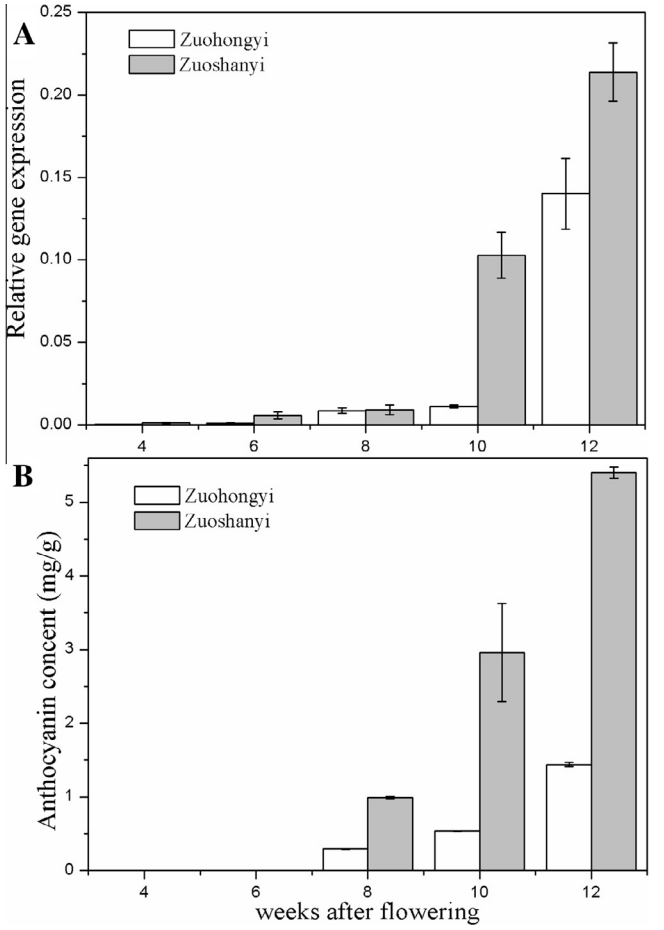

Fig. 6. The relationship between gene expression of *Va5GT* and accumulation of anthocyanidin bis-glucosides in grape berries of different cultivars at different developmental stages.

selected from wild resources, female) × 'Shuangqing' (*V. amurensis* Rupr., selected from wild resources, hermaphroditic), hermaphroditic] of homogeneous vigor were grown on south-north oriented rows in the experimental vineyard of China Agricultural University (N40°08′, E116°11′, altitude 31.3 m) in the suburbs of Beijing. The experiments were conducted in 2010, and the average daily temperatures in the main berry growing season ranged from 24.7 °C (June) to 26.5 °C (August), with mean relative humidity values ranging from 59.9% (June) to 63.9% (August). The rainfall from May to September was 410.8 mm in total. Berries of the two cultivars were collected at five developmental stages from June 14th (4 weeks after flowering) to September 8th (12 weeks after flowering, commercial harvest time) in 2010 at 2-week intervals. Samples were collected according to the methods described by Boulton et al. (1995) with some modifications. Three 100-berry samples were selected from at least seven 10-bunch selections at similar positions on 20 whole vine selections. The fresh samples were kept refrigerated in bags and then taken to the laboratory within one hour. Then, the grape skins were peeled from the berries by hand, and the skins and flesh parts were frozen in liquid N_2 and then stored separately at −80 °C until use.

Most monoglucosidic anthocyanins and bis-glucosidic anthocyanins were purchased from Polyphenols Laboratories (http://www.polyphenols.com/) (Norway). Malvidin-3-*O*-galactoside (**16**), cyanidin-3-*O*-rutinoside (**14**), UDP-glucose and UDP-galactose were purchased from Sigma–Aldrich (http://www.sigmaaldrich.com) (USA). RNase-free DNase, oligo $d(T)_{18}$ primers, dNTP mixture cloned ribonuclease inhibitor, pMD19-T vector and restriction endonucleases were purchased from Takara (http://www.takara.com.cn/) (Japan). M-MLV reverse transcriptase was purchased from Promega www.promega.com.cn/) (USA). All oligonucleotide primers were synthesized by Sangon Biotech (http://www.sangon.com/) (Shanghai, China), and PCR products were confirmed by sequencing by the same company. HPLC grade MeOH, HCO_2H, AcOH and MeCN were purchased from Fisher Scientific (http://www.thermo.com.cn) (USA).

4.2. RNA extraction and molecular cloning of Va5GT

High quality RNA for gene cloning was extracted from the skins of 'Zuoshanyi' (*V. amurensis* Rupr. cv.) grapes at veraison (8 weeks after flowering) according to the optimized and modified cetyl triethylammonium bromide (CTAB) protocol (He et al., 2009; Wen et al., 2005). Total RNA was treated with RNase-free DNase to remove the grape genomic DNA and then purified using the EZ-10 Spin Column RNA Purification Kit (Bio BasicINC, http://store.biobasic.com/).

Total RNA was reverse-transcribed using M-MLV reverse transcriptase and the oligo $d(T)_{18}$ primer. The first-strand of cDNA was synthesized at 42 °C for 1 h, and the reaction was terminated by heating at 72 °C for 5 min. The previously characterized full-length 'Regent' *Cha5GT* cDNA sequence was used to design the forward primer (5′-CACTTTCCACCTGAGACACC-3′) and the reverse primer (5′-CAGTACATCAAACGCCACTC-3′) for that PCR (Jánváry et al., 2009). Each PCR reaction tube contained 2 × Pfu PCR MasterMix, and the PCR was carried out at 94 °C for 10 min followed by 30 cycles of 94 °C for 30 s, 55 °C for 30 s, and 72 °C for 70 s and then a final extension at 72 °C for 5 min.

The PCR product was purified by agarose gel electrophoresis and then sub-cloned into the pMD19-T vector. The recombinant pMD19-T-*Va5GT* plasmid was then introduced into *E. coli* DH5α cells. The transformation was verified by colony PCR and double restriction endonuclease analysis of the extracted plasmids. Finally, the pMD19-T-*Va5GT* plasmid was sequenced from both sides of the inserted fragments. The DNA sequence was analyzed using ContigExpress and AlignX programs of the Vector NTI Advance 11 software suite (Invitrogen, http://www.invitrogen.com/). The nucleotide sequence alignments of *Va5GT* with other glycosyltransferase sequences and the subsequent phylogenetic analysis were performed using ClustalX (http://www.clustal.org/) and Mega 4 (http://www.megasoftware.net/).

4.3. Expression and purification of recombinant Va5GT

According to the sequence of *Va5GT* and the pET32a vector plasmid, two restriction sites (*Bam*HI and *Xho*I) were selected, and specific primers were designed and synthesized for amplifying the *Va5GT* gene: forward primer 5′-CGGGATCCATGGCGAATCCTCA CCCCCAT-3′ and reverse primer 5′-CCGCTCGAGTTTAATAACCTT GTATAACCTC-3′ (the restriction sites are underlined, and the start and stop codons are double-underlined). The PCR reaction was carried out using pMD19-T-*Va5GT* as the template. Then, the purified PCR products and the pET32a plasmid were double-digested with *Bam*HI and *Xho*I restriction endonucleases to construct the recombinant prokaryotic expression plasmid pET32a-*Va5GT,* which was then introduced into *E. coli* Rosetta (DE3) cells. The transformation was verified as mentioned above. A single colony of *E. coli* Rosetta (DE3) harboring the reconstructed plasmids was cultured at 37 °C in LB liquid medium containing 100 μg/ml ampicillin and then treated with IPTG (1 mM) to induce the expression of the fused protein. The recombinant protein was extracted from *E. coli* Rosetta (DE3) pellets, purified by Ni–NTA His-Bind Resin (Novagen, http://www.novagen.com/), concentrated by 10 kDa

MWCO centrifuge filter units (Millipore, http://www.merckmillipore.com/) and analyzed by sodium dodecyl sulfate–polyacrylamide gel electrophoresis (SDS–PAGE). Total protein concentration was determined by the Bradford method using bovine serum albumin (BSA) as the standard.

4.4. Recombinant Va5GT enzyme activity assays

Typically, recombinant Va5GT protein (2.5 μg), 1 mM donor substrate (UDP-glucose or UDP-galactose) and 0.5 mM acceptor substrate in K_3PO_4 buffer (100 mM, pH 7.0) were incubated at 25 °C for 20 min in a final volume of 100 μl. Different anthocyanins were used as acceptor substrates, including pelargonidin-3-*O*-glucoside (**2**), cyanidin-3-*O*-glucoside (**4**), delphinidin-3-*O*-glucoside (**6**), peonidin-3-*O*-glucoside (**8**), petunidin-3-*O*-glucoside (**10**), malvidin-3-*O*-glucoside (**12**), cyanidin-3-*O*-rutinoside (**14**) and malvidin-3-*O*-galactoside (**16**).

For determination of optimum temperature for enzymatic activity of Va5GT, 2.5 μg recombinant Va5GT enzyme, 1 mM UDP-glucose and 0.5 mM malvidin-3-*O*-glucoside (**12**) in a final assay volume of 100 μl were incubated at 10 °C, 15 °C, 20 °C, 25 °C, 30 °C, 35 °C and 40 °C for 20 min. K_2HPO_4–KH_2PO_4 buffers with a series of pH values, 3.0, 4.0, 5.0, 6.0, 7.0, 8.0, 9.0, 10.0 and 11.0, were used to determine the optimum pH value for the enzymatic activity of Va5GT, and this assay was performed at 25 °C for 20 min. Then, the linear relationship between enzyme activity and reaction time was assessed in a 100 μl reaction mixture consisting of 500 μM malvidin-3-*O*-glucoside (**12**) and 5 mM UDP-glucose in 100 mM K_3PO_4 buffer (pH 7.0) incubated at 25 °C for different times. For the determination of Va5GT kinetic parameters, all reaction mixtures were incubated for either 6 min or 10 min at 25 °C with a final reaction volume of 100 μl consisting of recombinant Va5GT protein (2.5 μg) and K_3PO_4 buffer (pH 7.0). For the acceptor substrates, each assay contained 5 mM UDP-glucose with different concentrations of malvidin-3-*O*-glucoside (**12**) ranging from 5 to 600 μM. The UDP-glucose kinetic parameters were determined with malvidin-3-*O*-glucoside (**12**) maintained at a constant concentration of 500 μM and a UDP-glucose concentration that varied from 0.05 to 2 mM.

4.5. Subcellular localization of Va5GT

To observe the subcellular localization of Va5GT, the *Va5GT* coding sequence was amplified using the forward primer 5′-CCGCTCGAGATGGCGAATCCTCACCCCCA-3′ and the reverse primer 5′-ACGCGTCGACTGATAACCTTGTATAACCTCAT-3′ (the restriction sites for *Xho*I and *Sal*I are underlined). The *Va5GT* ORF driven by the Cauliflower mosaic virus (CaMV) 35S promoter was fused upstream of GFP at the *Xho*I (5′-end) and *Sal*I (3′-end) sites in the pEZS-NL vector. A PYR1 protein tagged with mCherry was used as the positive marker for the observation of Va5GT's localization. Protoplasts were isolated from 4-week-old *Arabidopsis* (ecotype Columbia-0) leaves. The pEZS-NL-*Va5GT* and pMD19-T-*PYR1* recombinant vectors were transiently transformed into protoplasts by the PEG-Ca^{2+} method. The fluorescences of GFP and RFP were observed separately using a confocal laser scanning microscope (Nikon C1-Si, Japan) (Zhao et al., 2011).

4.6. Anthocyanin extraction from grape skins

According to a previously published method, the skin was peeled and immediately ground into a powder in liquid N_2 (He et al., 2010b). Grape skin powder (0.50 g) was immersed in MeOH (10 ml) containing 2% HCO_2H. The mixture was ultrasound sonicated for 10 min followed by shaking in the dark at 25 °C for 30 min at 150 rpm. The homogenate was centrifuged and the supernatant was collected. The residues were re-extracted four times. All of the supernatants were mixed, concentrated to dryness using a rotary evaporator and then redissolved in EtOH: H_2O (10 ml, 1:9 v/v, pH 3.7). Each sample was independently extracted twice.

4.7. HPLC–ESI–MS/MS analysis of anthocyanins

All of the resulting reaction mixtures and extracted suspensions were filtered through 0.22 μm cellulose acetate and nitrocellulose filters (MEMBRANA, http://www.membrana.com/) (Germany) separately prior to HPLC–ESI–MS/MS analysis. Each sample was then independently analyzed twice.

The analyses of anthocyanins in the enzyme assays and in the grape skin extracts were carried out according to the method reported by Han et al. (2008) with little alteration. An Agilent 1100 series LC-MSD trap VL (http://www.agilent.com) equipped with a G1379A Degasser, a G1311A QuatPump, a G1313A ALS, a G1316A Column thermostat, a G1315B DAD and a Kromasil-C18 column (250 × 4.6 mm, 5 mm) was used. The solvents were as follows: (A) 2% HCO_2H in H_2O; and (B) MeCN containing 2% HCO_2H. The flow rate was 1.0 ml/min, and the solvent gradients used were as follows: from 6% to 10% B over 4 min, from 10% to 25% B over 8 min, isocratic 25% B for 1 min, from 25% to 40% B over 7 min, from 40% to 60% B over 15 min, from 60% to 100% B over 5 min and from 100% to 6% B over 5 min. The injection volume was 30 μl, and the detection wavelength was 525 nm. The column temperature was 50 °C. The MS conditions were as follows: ESI interface, positive ion mode, 35 psi nebulizer pressure, 10 ml/min drying N_2 flow rate, 350 °C drying N_2 temperature, capillary voltage 3000 V and scans at *m*/*z* 100–1000. All analyses were performed in duplicate.

4.8. Analysis of the transcriptional expression of Va5GT during berry development

RNA was extracted from the berry skins of 'Zuoshanyi' and 'Zuohongyi' grapes at all developmental stages. Then, RNA samples were used for reverse transcription to produce the corresponding cDNAs. The relative expression of *Va*5GT was monitored by real-time PCR with the following gene specific primers: forward 5′-AGGTGATTGGAATTGGTTATGG-3′ and reverse 5′-GGCATTCTTTCTC ATTTCTTGG-3′. *VvUbiquitin1* was chosen as the internal reference (TIGR database: TC32075) and was amplified with the following primers: forward 5′-TGGTATTATTGAGCCATCCTT-3′ and reverse 5′-ACCTCCAATCCAGTCATCTAC-3′. The amplification efficiency of the primers used in the real-time PCR analysis was tested and was found to be the same when serial dilutions were used. The PCR reaction tubes contained 5 μl SYBR Green RT-PCR Master Mix (Takara, http://www.takara.com.cn/) (Japan), 0.2 μl 50 × ROX Reference Dye, 4.5 μl ddH_2O, 1/6 μl cDNAs and 1/3 μl primers mixture (10 μM). The PCR parameters including pre-denaturation at 95 °C for 30 s and 40 cycles of 95 °C for 10 s and 60 °C for 30 s. *VvUbiquitin1* was chosen for the normalization of gene expression. The gene expression measurements of *Va5GT* and *VvUbiquitin1* were repeated in triplicate and were relatively quantified by the $2^{-\Delta Ct}$ method (Bogs et al., 2005), with ΔCt equal to the cycle threshold of *Va5GT* – the cycle threshold of *VvUbiquitin*.

Acknowledgements

We greatly thank Prof. Wilfried Schwab (Biomolecular Food Technology, Technische Universität München, Germany) for providing us with the cDNA sequences of *Cha5GT* and *Dia5GT*. We thank Prof. Da-Peng Zhang (Protein Science Laboratory of the Ministry of Education, School of Life Sciences, Tsinghua

University, China), who provided us with the pEZS-NL and the pMD19-T-*PYR1* vectors, as well as related experimental supports and suggestions for our research. Besides, this research was supported by the China Agriculture Research System (CARS-30) and the Research Fund for the Doctoral Program of Higher Education of China (20130008120027).

Appendix A. Supplementary data

Supplementary data associated with this article can be found, in the online version, at http://dx.doi.org/10.1016/j.phytochem.2015.06.023.

References

Bogs, J., Downey, M.O., Harvey, J.S., Ashton, A.R., Tanner, G.J., Robinson, S.P., 2005. Proanthocyanidin synthesis and expression of genes encoding leucoanthocyanidin reductase and anthocyanidin reductase in developing grape berries and grapevine leaves. Plant Physiol. 139, 652–663.

Boulton, R., Singleton, V., Bisson, L., Kunkee, R., 1995. Selection of state of ripeness for harvest and harvesting. In: Principles and Practices of Winemaking. International Thomson Publishing, New York, pp. 52–60.

Cartwright, A.M., Lim, E.K., Kleanthous, C., Bowles, D.J., 2008. A kinetic analysis of regiospecific glucosylation by two glycosyltransferases of *Arabidopsis thaliana*: domain swapping to introduce new activities. J. Biol. Chem. 283, 15724–15731.

Coutinho, P.M., Deleury, E., Davies, G.J., Henrissat, B., 2003. An evolving hierarchical family classification for glycosyltransferases. J. Mol. Biol. 328 (2), 307–317.

Downey, M.O., Dokoozlian, N.K., Krstic, M.P., 2006. Cultural practice and environmental impacts on the flavonoid composition of grapes and wine: a review of recent research. Am. J. Enol. Vitic. 57, 257–268.

Emanuelsson, O., Brunak, S., von Heijne, G., Nielsen, H., 2007. Locating proteins in the cell using TargetP, SignalP and related tools. Nat. Protoc. 2, 953–971.

Felle, H.H., 2005. PH regulation in anoxic plants. Ann. Bot. 96, 519–532.

Ford, C.M., Boss, P.K., Hoj, P.B., 1998. Cloning and characterization of *Vitis vinifera* UDP-glucose: flavonoid 3-*O*-glucosyltransferase, a homologue of the enzyme encoded by the maize *Bronze*-1 locus that may primarily serve to glucosylate anthocyanidins *in vivo*. J. Biol. Chem. 273, 9224–9233.

Fujiwara, H., Tanaka, Y., Yonekura-Sakakibara, K., Fukuchi-Mizutani, M., Nakao, M., Fukui, Y., Yamaguchi, M., Ashikari, T., Kusumi, T., 1998. CDNA cloning, gene expression and subcellular localization of anthocyanin 5-aromatic acyltransferase from *Gentiana triflora*. Plant J. 16 (4), 421–431.

Hall, D., De Luca, V., 2007. Mesocarp localization of a bi-functional resveratrol/hydroxycinnamic acid glucosyltransferase of Concord grape (*Vitis labrusca*). Plant J. 49, 579–591.

Hall, D., Yuan, X.X., Murata, J., De Luca, V., 2012. Molecular cloning and biochemical characterization of the UDP-glucose: flavonoid 3-*O*-glucosyltransferase from Concord grape (*Vitis labrusca*). Phytochemistry 74, 90–99.

Han, F.L., Zhang, W.N., Pan, Q.H., Zheng, C.R., Chen, H.Y., Duan, C.Q., 2008. Principal component regression analysis of the relation between CIELAB color and monomeric anthocyanins in young Cabernet Sauvignon wines. Molecules 13, 2859–2870.

He, F., Fang, X.X., Hu, M., Pan, Q.H., Shi, Y., Duan, C.Q., 2009. Preparation and biological application of antibodies against leucoanthocyanidin reductase and anthocyanidin reductase from grape berry. Vitis 48, 69–75.

He, F., Mu, L., Yan, G.L., Liang, N.N., Pan, Q.H., Wang, J., Reeves, M.J., Duan, C.Q., 2010a. Biosynthesis of anthocyanins and their regulation in colored grapes. Molecules 15, 9057–9091.

He, J.J., Liu, Y.X., Pan, Q.H., Cui, X.Y., Duan, C.Q., 2010b. Different anthocyanin profiles of the skin and the pulp of Yan73 (Muscat Hamburg × Alicante Bouschet) grape berries. Molecules 15, 1141–1153.

Heller, W., Forkmann, G., 1993. The flavonoids: advances in research since 1986. In: Harborne, J.B. (Ed.), Biosynthesis of Flavonoids, pp. 499–535.

Hrazdina, G., Wagner, G.J., 1985. Metabolic pathways as enzyme complexes: evidence for the synthesis of phenylpropanoids on membrane associated enzyme complexes. Arch. Biochem. Biophys. 237, 88–100.

Hrazdina, G., Wagner, G.J., Siegelman, H.W., 1978. Subcellular localization of enzymes of anthocyanin biosynthesis in protoplasts. Phytochemistry 17, 53–56.

Hrazdina, G., Parsons, G.F., Mattick, L.R., 1984. Physiological and biochemical events during development and maturation of grape berries. Am. J. Enol. Vitic. 35, 220–227.

Hughes, J., Hughes, M.A., 1994. Multiple secondary plant product UDP-glucose glucosyltransferase genes expressed in cassava (Manihot esculenta Crantz) cotyledons. Mitochond DNA 5 (1), 41–49.

Hugueney, P., Provenzano, S., Verriès, C., Ferrandino, A., Meudec, E., Batelli, G., Merdinoglu, D., Cheynier, V., Schubert, A., Ageorges, A., 2009. A novel cation-dependent *O*-methyltransferase involved in anthocyanin methylation in grapevine. Plant Physiol. 150 (4), 2057–2070.

Jánváry, L., Hoffmann, T., Pfeiffer, J., Hausmann, L., Topfer, R., Fischer, T.C., Schwab, W., 2009. A double mutation in the anthocyanin 5-*O*-glucosyltransferase gene disrupts enzymatic activity in *Vitis vinifera* L. J. Agric. Food Chem. 57, 3512–3518.

Kiselev, K.V., Dubrovina, A.S., Veselova, M.V., Bulgakov, V.P., Fedoreyev, S.A., Zhuravlev, Y.N., 2007. The rolB gene-induced overproduction of resveratrol in *Vitis amurensis* transformed cells. J. Biotechnol. 128, 681–692.

Kovács, L.G., Byers, P.L., Kaps, M.L., Saenz, J., 2003. Dormancy, cold hardiness, and spring frost hazard in *Vitis amurensis* hybrids under continental climatic conditions. Am. J. Enol. Vitic. 54, 8–14.

Kubo, A., Arai, Y., Nagashima, S., Yoshikawa, T., 2004. Alteration of sugar donor specificities of plant glycosyltransferases by a single point mutation. Arch. Biochem. Biophys. 429, 198–203.

Martin, C., Gerats, T., Jordan, B., 1993. The control of flower coloration. The molecular biology of flowering. CIB International, Wallingford, pp. 219–255.

Matsuba, Y., Sasaki, N., Tera, M., Okamura, M., Abe, Y., Okamoto, E., Nakamura, H., Funabashi, H., Takatsu, M., Saito, M., Matsuoka, H., Nagasawa, K., Ozeki, Y., 2010. A novel glucosylation reaction on anthocyanins catalyzed by acyl-glucose-dependent glucosyltransferase in the petals of carnation and delphinium. Plant Cell. 22, 3374–3389.

Mazza, G., 1995. Anthocyanins in grapes and grape products. Crit. Rev. Food Sci. Nutr. 35, 341–371.

Mazzuca, P., Ferranti, P., Picariello, G., Chianese, L., Addeo, F., 2005. Mass spectrometry in the study of anthocyanins and their derivatives: differentiation of *Vitis vinifera* and hybrid grapes by liquid chromatography/electrospray ionization mass spectrometry and tandem mass spectrometry. J. Mass Spectrom. 40, 83–90.

Montefiori, M., Espley, R.V., Stevenson, D., Cooney, J., Datson, P.M., Saiz, A., Atkinson, R.G., Hellens, R.P., Allan, A.C., 2011. Identification and characterisation of F3GT1 and F3GGT1, two glycosyltransferases responsible for anthocyanin biosynthesis in red-fleshed kiwifruit (*Actinidia chinensis*). Plant J. 65, 106–118.

Nakatsuka, T., Sato, K., Takahashi, H., Yamamura, S., Nishihara, M., 2008. Cloning and characterization of the UDP-glucose:anthocyanin 5-*O*-glucosyltransferase gene from blue-flowered gentian. J. Exp. Bot. 59, 1241–1252.

Neumann, K., Eibach, R., Zyprian, E., Hausmann, L., Töpfer, R., 2006. Development of a molecular marker for an anthocyanin 5-O-glucosyltransferase homologous gene of Vitis ssp. correlated with anthocyanin 3,5-diglucoside formation in berry skin. In: IX International Conference on Grape Genetics and Breeding, vol. 827, pp. 457–460.

Offen, W., Martinez-Fleites, C., Yang, M., Kiat-Lim, E., Davis, B.G., Tarling, C.A., Ford, C.M., Bowles, D.J., Davies, G.J., 2006. Structure of a flavonoid glucosyltransferase reveals the basis for plant natural product modification. EMBO J. 25, 1396–1405.

Ogata, J., Sakamoto, T., Yamaguchi, M., Kawanobu, S., Yoshitama, K., 2001. Isolation and characterization of anthocyanin 5-*O*-glucosyltransferase from flowers of *Dahlia variabilis*. J. Plant Physiol. 158, 709–714.

Owens, D.K., McIntosh, C.A., 2009. Identification, recombinant expression, and biochemical characterization of a flavonol 3-*O*-glucosyltransferase clone from *Citrus paradisi*. Phytochemistry 70, 1382–1391.

Park, S.Y., Fung, P., Nishimura, N., Jensen, D.R., Fujii, H., Zhao, Y., Lumba, S., Santiago, J., Rodrigues, A., Chow, T.F.F., Alfred, S.E., Bonetta, D., Finkelstein, R., Provart, N.J., Desveaux, D., Rodriguez, P.L., McCourt, P., Zhu, J.K., Schroeder, J.I., Volkman, B.F., Cutler, S.R., 2009. Abscisic acid inhibits type 2C protein phosphatases via the PYR/PYL family of START proteins. Science 324 (5930), 1068–1071.

Shewfelt, A.L., Ahmed, E., 1966. The nature of the anthocyanin pigments in South Carolina Concord grapes. South Carolina Agricultural Experiment Station, Clemson University.

Sparvoli, F., Martin, C., Scienza, A., Gavazzi, G., Tonelli, C., 1994. Cloning and molecular analysis of structural genes involved in flavonoid and stilbene biosynthesis in grape (*Vitis vinifera* L.). Plant Mol. Biol. 24, 743–755.

Tanaka, Y., Tsuda, S., Kusumi, T., 1998. Metabolic engineering to modify flower color. Plant Cell Physiol. 39 (11), 1119–1126.

Vogt, T., Jones, P., 2000. Glycosyltransferases in plant natural product synthesis: characterization of a supergene family. Trends Plant Sci. 5, 380–386.

Wan, Y., Schwaninger, H., He, P., Wang, Y., 2007. Comparison of resistance to powdery mildew and downy mildew in Chinese wild grapes. Vitis 46, 132.

Wen, P.F., Chen, J.Y., Kong, W.F., Pan, Q.H., Wan, S.B., Huang, W.D., 2005. Salicylic acid induced the expression of phenylalanine ammonia-lyase gene in grape berry. Plant Sci. 169, 928–934.

Winkel-Shirley, B., 1999. Evidence for enzyme complexes in the phenylpropanoid and flavonoid pathways. Physiol. Plant. 107, 142–149.

Winkel-Shirley, B., 2001. Flavonoid biosynthesis. A colorful model for genetics, biochemistry, cell biology, and biotechnology. Plant Physiol. 126, 485–493.

Winkel-Shirley, B., 2004. Metabolic channeling in plants. Annu. Rev. Plant Biol. 55, 85–107.

Yamazaki, M., 1999. Molecular cloning and biochemical characterization of a novel anthocyanin 5-*O*-glucosyltransferase by mRNA differential display for plant forms regarding anthocyanin. J. Biol. Chem. 274, 7405–7411.

Yonekura-Sakakibara, K., Nakayama, T., Yamazaki, M., Saito, K., 2009. Modification and stabilization of anthocyanins. In: Gould, K.S., Davies, K.M., Winefield, C. (Eds.), Anthocyanin Biosynthesis, Functions, and Applications. Springer Science and Business Media, New York, pp. 169–190.

Zhao, Q., Duan, C.Q., Wang, J., 2010. Anthocyanins profile of grape berries of *Vitis amurensis*, its hybrids and their wines. Int. J. Mol. Sci. 11, 2212–2228.

Zhao, R., Sun, H.L., Mei, C., Wang, X.J., Yan, L., Liu, R., Zhang, X.F., Wang, X.F., Zhang, D.P., 2011. The *Arabidopsis* Ca(2+)-dependent protein kinase CPK12 negatively regulates abscisic acid signaling in seed germination and post-germination growth. New Phytol. 192, 61–73.

Zhu, L., Zhang, Y.L., Lu, J., 2012. Phenolic contents and compositions in skins of red wine grape cultivars among various genetic backgrounds and originations. Int. J. Mol. Sci. 13, 3492–3510.